NASA
Technical Memorandum 101356

AVSCOM
Technical Report 88-C-027

Properties of Silicon Carbide Fiber-Reinforced Silicon Nitride Matrix Composites

Ramakrishna T. Bhatt
Propulsion Directorate
U.S. Army Aviation Research and Technology Activity—AVSCOM
Lewis Research Center
Cleveland, Ohio

Presented at the
International Conference on Whisker- and Fiber-Toughened Ceramics
sponsored by the American Society for Metals
Oak Ridge, Tennessee, June 6-9, 1988

NASA

US ARMY
AVIATION
SYSTEMS COMMAND
AVIATION R&T ACTIVITY

PROPERTIES OF SILICON CARBIDE FIBER-REINFORCED SILICON NITRIDE MATRIX COMPOSITES

Ramakrishna T. Bhatt
Propulsion Directorate
U.S. Army Aviation Research and Technology Activity - AVSCOM
Lewis Research Center
Cleveland, Ohio 44135

SUMMARY

The mechanical properties of NASA Lewis Research Center developed SiC/RBSN composites and their thermal and environmental stability have been studied. The composites consist of nearly 30 vol % of aligned 142 μm diameter chemically vapor-deposited SiC fibers in a relatively porous silicon nitride matrix. In the as-fabricated condition, the unidirectional and two-dimensional composites exhibited metal-like stress-strain behavior, graceful failure, and showed improved properties when compared with unreinforced matrix of comparable density. Furthermore, the measured room temperature tensile properties were relatively independent of tested volume and were unaffected by artificial notches normal to the loading direction or by thermal shocking from temperatures up to 1100 °C. The four-point bend strength data measured as a function of temperature to 1400 °C in air showed that as-fabricated strength was maintained to 1200 °C. At 1400 °C, however, nearly 15 percent loss in strength was observed. Measurement of room temperature tensile strength after 100 hr exposure at temperatures to 1400 °C in a nitrogen environment indicated no loss from the as-fabricated composite strength. On the other hand, after 100 hr exposure in flowing oxygen at 1200 and 1400 °C, the composites showed ~40 percent loss from their as-fabricated ultimate tensile strength. Those exposed between 400 to 1200 °C showed nearly 60 percent strength loss. Oxidation of the fiber/matrix interface as well as internal oxidation of the porous Si_3N_4 matrix are likely mechanisms for strength degradation. The excellent strength reproducibility, notch insensitivity, and high temperature strength of the composite makes it an ideal candidate for advanced heat engine applications provided coating or densification methods are developed to avoid internal oxidation attack.

E-4386

INTRODUCTION

Silicon based monolithic ceramic materials are potential candidates for advanced heat engine applications. However these materials are not utilized as structural components because of their flaw sensitivity, poor reliability, and brittle fracture behavior. Reinforcement of these materials by particulates, whiskers, or by continuous fibers should improve their reliability. Studies (refs. 1 and 2) have shown that the addition of SiC and TiN particulates or SiC whiskers to Si_3N_4 matrix can result in a two-fold increase in fracture toughness, but final materials still exhibited brittle behavior. On the other hand, continuous fiber reinforcements offer certain advantages over particulate or whisker reinforcements. First, high modulus, high strength, small diameter ceramic fiber reinforcements in a ceramic matrix can bridge matrix flaws and delay the onset of matrix fracture to a much higher strain and stress level than the unreinforced matrix. Second, proper choice of fiber

reinforcement and proper control of fiber/matrix bond will permit the matrix cracks to go around the fibers and not through them. This allows the fibers to bear the load beyond the matrix fracture and prevent catastrophic failure of the material at the instant of matrix fracture.

In its pursuit of low density, strong, tough, reliable ceramic materials for structural components, NASA Lewis has developed a fiber-reinforced silicon-based ceramic composite system. In this paper the mechanical properties, flaw sensitivity, and environmental stability of this composite system are discussed.

EXPERIMENTAL

Materials

The starting materials for the SiC/RBSN composite fabrication were SiC fiber monofilaments and high purity silicon powder. The SiC fiber monofilaments were obtained from Textron Specialty Materials. These fibers were produced by chemical vapor deposition from methyl-trichlorosilane onto a heated carbon substrate. At the outer surface of the SiC sheath, the manufacturer provides different surface coatings which serve several purposes. They can heal surface irregularities on the SiC substrate, thereby providing abrasion resistance and improved fiber strength. They can also provide a weak interface for matrix crack deflection. A schematic diagram of the cross section of the CVD SiC fiber is shown in figure 1(a). The fiber consists of a sheath with an outer diameter of 142 μm surrounding a pyrolitic graphite-coated carbon core with diameter of 37 μm. The fiber used for SiC/RBSN composite fabrication contained two layers of carbon-rich surface coating. Each layer is a mixture of amorphous carbon and SiC. The elemental composition of the fiber surface coating is shown in figure 1(b). The manufacturer designates this fiber as double coated SCS-6 SiC fiber. This fiber was developed for metal matrix composites. The SCS-6 fibers tested from different fiber spools as well as different sections of the same spool showed large scatter in room temperature tensile strength. The average room temperature tensile strength and the elastic modulus of the fiber are 3.8 ± 0.7 and 390 GPa respectively (ref. 3).

For the silicon nitride matrix, high purity silicon powder obtained from Union Carbide was used. The as-received powder contained large agglomerates and required attrition milling to reduce its particle size and to improve its reactivity to nitrogen during a later nitridation step. The attrition milling procedure and impurity analysis of the attrition milled powder were discussed elsewhere (ref. 4). The average particle size of the attrition milled powder was 0.03 μm.

Composite Fabrication

The starting materials for composite fabrication were SiC fiber mats and silicon powder cloth. The block diagram shown in figure 2 gives the steps involved in composite fabrication. The details of the composite fabrication procedure were described in reference 5. To describe the composite fabrication briefly, first the SiC fiber mats were prepared by winding the SiC fibers with desired spacing on a cylindrical drum. The fiber spacing used depended on the desired fiber volume fraction in the composite. The fiber mats were coated with fugitive polymer binder to maintain the fiber spacing. After drying, the fiber mats were cut to 125 by 50 mm pieces.

For silicon cloth preparation, the attrition-milled silicon powder was mixed with polymer fugitive binder and an organic solvent until a dough of desirable consistency was obtained. This dough was rolled to the desired thickness to produce silicon cloth. The thickness of the cloth determined the matrix volume fraction in the composite. The silicon cloth was cut into 125 by 50 mm pieces.

For composite preform fabrication, the fiber mat and the silicon cloth were alternately stacked in a metal die and hot pressed in vacuum to remove the fugitive polymer binder at an appropriate temperature and pressure. The resultant composite preform was transferred to a nitridation furnace and nitrided to convert silicon to silicon nitride matrix. Using this fabrication method unidirectional $[0]_8$ and cross-plied $[0/90]_S$ composites, and unreinforced RBSN were prepared. Typical dimensions of composite plates were 125 by 50 by 2 mm.

Each composite plate contained ~30 vol % of SiC fibers. The silicon nitride matrix was relatively porous and contained ~30 vol % porosity. The average composite density and matrix pore size were 2.0 gm/cc and 0.02 μm, respectively. The composite density was measured by the Archimedes method using methyl ethyl ketone liquid and pore size measurements were made by mercury porosimeter. A photomicrograph of the cross section of a 30 percent SiC/RBSN composite shown in figure 3 indicates the distribution of the SiC fibers in the RBSN matrix and the substructures contained within the SiC fibers. A higher magnification photograph of the composite cross section shown in figure 4 shows the interfacial region between the SiC fiber and RBSN matrix and the two layers contained in the carbon-rich fiber surface coating.

RESULTS

Typical room temperature tensile stress-strain curves for the unidirectional $[0]_8$ and cross plied $[0/90]_S$ composites are shown in figure 5. The stress-strain curves for the $[90]_8$ composites and the unreinforced RBSN matrix are included in figure 5 for comparison purposes. In general, the stress-strain curves for both the $[0]_8$ and $[0/90]_S$ composites showed three distinct regions: an initial linear elastic region, followed by a nonlinear region, and then a second linear region. The nonlinear region originated with the onset of matrix cracking normal to the loading direction. With continued stressing additional matrix cracks were formed; and at the end of the nonlinear range, regularly spaced matrix cracks were seen. The average matrix crack spacing for $[0]_8$ was 0.8 ± 0.2 mm. Using measured values of the average matrix crack spacing, the first matrix cracking stress, and the elastic properties of the fiber and the matrix, it is possible to calculate the interfacial shear strength between the fiber and the matrix from composite theory (ref. 6). Beyond the nonlinear region, a second linear region was observed until final fiber-controlled failure of the composite occurred. On the other hand, the stress-strain curves for the monolithic RBSN and the $[90]_8$ composites showed only the initial linear region. Both these materials showed no evidence of strain capability beyond matrix fracture. Examination of broken tensile specimens of $[0]_8$ and $[0/90]_S$ composites showed a broom-like fracture surface with minimal matrix around the fibers. Optical photographs of representative fractured tensile specimens for both of these composites is shown in figure 6.

Comparison of the stress-strain curves in figure 5 provided additional information. First, the composite displayed anisotropy in in-plane properties. Second, the matrix fracture strain for the $[0]_8$ composites was slightly higher than that of the unreinforced RBSN matrix. This indicates that reinforcement of RBSN by large diameter SiC fibers did not significantly affect matrix fracture strain. This is in contrast to the microcrack bridging effect seen in small diameter carbon fiber reinforced glass composites (ref. 6). Third, the composite strain at which the matrix fractured for the $[0]_8$ composites was nearly equivalent to that for the $[0/90]_S$ composites. This suggests that ply lay-up in the composite has minimum influence on the matrix fracture strain. Lastly, the matrix fractures at ~0.03 percent strain for the $[90]_8$, but at ~0.1 percent for the $[0/90]_S$ composites. This indicates that coupling stresses between [0] and [90] plies restricts fracture of the [90] plies in $[0/90]_S$.

The room temperature elastic and fracture properties measured from the stress-strain curves of the unidirectional and cross-plied composites are listed in table I. The interfacial shear strength, in-plane shear strength, and the fracture toughness values for the composites are also included in the table I. The measurement of these property data are discussed in the following sections. Each data entry in the table represents an average of five tests. The scatter in data represents two standard deviations. The large scatter in the ultimate tensile strength for the composite is due to large variation in the ultimate tensile strength of SiC fibers seen from one fiber spool to another as well as within a fiber spool itself. On the other hand the scatter in matrix related properties reflects batch to batch variation in fabrication.

Interfacial Shear Strength

Interfacial shear strength between the SiC fibers and RBSN matrix was calculated from the Aveston, Cooper, and Kelly theory (ref. 6). The interfacial shear strength, τ, between the fiber and the matrix can be estimated from the equation

$$\tau = \sigma_c^f D/[2.98 \times V_f(1 + E_f V_f/E_m V_m)]$$

Here σ_c^f is the composite stress corresponding to the first matrix crack, x is the average matrix crack spacing, D is the fiber diameter, E_f is the fiber modulus, E_m is the matrix modulus, and V_f is the fiber volume fraction.

Using the values of x = 0.8 mm, σ_c^f = 227 MPa, E_m = 110 MPa, V_f = 0.3, D = 142 μm, E_f = 390 MPa (ref. 3) in the equation, the calculated value of mean interfacial shear strength was 18 MPa.

Interlaminar Shear Strength

For interlaminar shear strength measurement, double notched shear test specimens were used. These specimens were 27 mm long with cross section of 6 by 6 mm. The specimen contained two 1 mm wide, 3 by 6 mm notches which were machined from the opposite faces of the specimen, 6 mm from each end. The specimens were tested in compression until failure. The interlaminar shear strength was then calculated from the maximum failure load and the shearing

area. The average interlaminar shear strength for uniaxially reinforced SiC/RBSN was 40 MPa.

Fracture Toughness

The fracture toughness for unidirectionally reinforced SiC/RBSN composite system was measured at room temperature using the notched beam method. This method was particularly chosen due to ease of specimen preparation compared to other methods such as the double torsion and cantilever beam. Specimen dimensions used were 50 by 6 by 6 mm. The center of the specimen contained a rectangular notch of dimensions 6 by 3 by 0.7 mm. The notch depth to specimen thickness ratio was 0.5 in all cases. The K calibration equation for the notched specimens was used from reference 7. For K_I measurement, the specimens were tested in three-point bend. During bend testing, cracks were formed initially normal to the notch tip and then these cracks grew along the fiber/matrix interface. With continued loading, cracks were formed parallel to the notch tip. At maximum load, the specimen deflected in the form of a U-shape, keeping its integrity. Even at maximum load level, the cracks propagating from the notch tip did not reached the compression side of the specimen. In contrast a notched monolithic ceramic under similar testing condition would break to pieces upon reaching the maximum stress. The fracture toughness was measured based on the load required for initial damage to specimens at the point of nonlinearity on the load-deflection curve. The measured K_I value for unidirectionally reinforced SiC/RBSN composite was 13 MPa $m^{-1/2}$. This value is nearly three times the reported K_I value of 4 MPa $m^{-1/2}$ for hot pressed Si_3N_4 (ref. 8).

Effect of Tested Volume on Strength

The influence of tested volume on the room temperature tensile properties of $[0]_8$ composites was determined by varying the gauge length from 12 to 127 mm. The properties measured were the matrix cracking stress and the ultimate composite strength. The results in terms of tested volume are plotted in figure 7. The data represents an average of five specimens. Included in figure 7 are the tensile strength results for hot-pressed Si_3N_4 (refs. 9 and 10).

Comparison of the data indicates that the first matrix cracking stress and the ultimate tensile strength for the composite is relatively independent of the tested volume, whereas the tensile strength of hot pressed Si_3N_4 varies inversely with the tested volume. Since monolithic ceramics are linearly elastic material until fracture, their strengths are governed by the largest flaw present in the tested volume. As the test volume increased, the probability for the presence of a larger flaw also increased. Therefore, the strength of monolithic ceramics decreases with increasing volume. On the other hand, the volume independent strength behavior for composites suggests that the strength of the composite does not depend on the largest flaw formed during fabrication or during specimen preparation, but depends on the complex interaction of local stress fields around the flaws and their growth due to global stresses. The implication of this finding is that for applications requiring large material volumes such as turbine blades or rotors the strength of SiC/RBSN composites may be better than that of commercially available dense hot pressed Si_3N_4.

Effect of Notches on Strength

In order to determine the behavior of SiC/RBSN composites under notched conditions, tensile specimens of $[0]_8$ and $[0/90]_S$ composites were notched at the center of specimen gauge section across the width. The tensile specimens were of same dimensions as those used for other tensile tests. Notches were machined to a depth of 3 mm using a diamond impregnated metal saw. Specimens contained either single or two opposing notches. The strength data for the notched and unnotched specimens are tabulated in table II. Results indicate that the strength properties of the composite are unaffected by notches. This composite behavior is quite different from that of monolithic ceramic materials where machined notches are known to have significant effect on their strength. This is another indication of the improved toughness of SiC/RBSN composites.

Effect of Thermal Shocking on Strength

The thermal shock resistance of uniaxially reinforced SiC/RBSN composites was evaluated using the water quench method. In this method the composites were first heated at temperatures to as high as 1100 °C in air for 15 min and then quenched in cold water. The effect of quenching on the room temperature tensile and bend properties was measured. The bend test specimens were of dimensions 50 by 6 by 22 mm. The bend specimens were tested in a four-point bend fixture having an outer and inner span of 40 and 20 mm, respectively. The dimensions of the tensile specimens were the same as described previously. The room temperature bend and tensile data for thermally shocked and as-fabricated composites are shown in figure 8. Included in figure 8 for comparison purposes are the four-point bend strength results for thermally shocked unreinforced monolithic RBSN (NC-350).

The results indicate that the room temperature ultimate tensile strength and the first matrix cracking stress values for the composite quenched from temperatures to 1100 °C were similar to those for the as-fabricated composites. On the other hand, the bend test results indicate loss of ultimate bend strength after quenches from above 600 °C. The bend strength loss behavior for the quenched unreinforced RBSN appeared similar to that for the composite, but for unreinforced RBSN, the strength loss occurred after quenches from temperatures above 425 °C which is 175 °C less than that observed for the composite. Although thermal shocking did damage to the composite, probably by microcracking of the matrix, it did not affect the tensile properties of the composite. From these results it can also be concluded that SiC/RBSN composites have better thermal shock resistance than the unreinforced RBSN and thus better toughness or flaw tolerance.

Thermal and Environmental Stability

Elevated Temperature Strength. - Four-point bend tests of SiC/RBSN composites were performed at temperatures from 25 to 1400 °C in air. These tests were performed at a depth to span ratio of 25:1. The ultimate bend strength data for the unidirectionally reinforced SiC/RBSN composite at 25, 1200, and 1400 °C are shown in figure 9. For comparison purposes, included in figure 9 are the elevated temperature bend strength data reported in the literature for hot pressed Si_3N_4 (ref. 11), unreinforced RBSN (ref. 11), and one-dimensional SEP SiC/composites (ref. 12). In making this comparison, it was assumed that

all of these materials failed by tensile fracture. The advantages of fiber reinforcement are apparent from comparison of the RBSN and composite data. The SiC/RBSN composites retained their as-fabricated strength at 1200 °C. At 1400 °C, however, a small loss in strength was observed. At room temperature, the hot pressed Si_3N_4 showed strength similar to that of the SiC/RBSN composites, but at 1200 and 1400 °C the SiC/RBSN composites retained a greater fraction of their as-fabricated strength than the hot pressed Si_3N_4. Finally, in the as-fabricated condition, the one-dimensional SEP SiC/SiC composites showed strength significantly lower than the SiC/RBSN composites, and at 1400 °C their strength decreased by 50 percent.

Environmental Stability

To investigate their environmental stability, the composite specimens were heat treated in flowing oxygen and in nitrogen environments for 100 hr at temperatures to 1400 °C and then tensile tested at room temperature. The specimen dimensions used were the same as those for other tensile tests used in this study. The variation of the matrix cracking stress and the ultimate tensile strength as a function of heat treating temperature are shown in figure 10. For the nitrogen treatment, as-fabricated strength was maintained from 25 to 1400 °C. In an oxidizing environment, however, an entirely different behavior was observed. The first matrix cracking stress values for the composites heat treated at 400, 1200, and 1400 °C were similar to those displayed by the composites in as-fabricated condition, but in the intermediate temperature range between 400 to 1200 °C, the first matrix cracking stress decreased initially with increasing exposure temperature up to 600 °C and then leveled off to a value of 120 MPa from 600 to 1000 °C. Beyond 1000 °C, it increased to a value corresponding to that of as-fabricated composites.

The variation of ultimate tensile strength of the composite with heat treatment temperature was similar to that observed for the first matrix crack stress. Although the composite lost nearly 60 percent of its as-fabricated strength after exposures in the intermediate temperatures (i.e, between 400 and 1200 °C), it lost only 40 percent of its strength at 1200 and 1400 °C. Comparison of the nitrogen and oxygen data indicates that the as-fabricated strengths for the composites used for the nitrogen treatment were appreciably higher than those for the oxidizing treatment. This difference is attributed to the differences in average ultimate tensile strength of the fibers used for composite fabrication. The higher the average tensile strength of the fiber spool used, the higher will be the average tensile strength of the as-fabricated composite. Data presented in figure 11 clearly indicates that in an oxidizing environment the composite shows strength degradation above 400 °C. A detailed discussion of the strength degrading mechanisms is beyond the scope of this paper and is given in reference 13. This reference identifies three mechanisms for the strength degradation. They are oxidation of the fiber/matrix interface, oxidation of the porous Si_3N_4, and intrinsic strength degradation of the SiC fibers. At low temperatures between 400 to 800 °C, where oxidation of porous Si_3N_4 is not kinetically favorable, oxygen could diffuse through the porous matrix and oxidize the carbon coating at the fiber/matrix interface. This reaction decouples the fiber from the matrix, causing loss of load transfer and loss of strength. In the temperature range between 800 to 1200 °C, where internal oxidation of the porous Si_3N_4 is prevalent, both reactions - formation of silica in the Si_3N_4 pores and oxidation of the fiber/matrix interface - occur simultaneously. Beyond 1200 °C, rapid oxidation of the porous Si_3N_4 matrix allows

formation of dense silica on the composite surface which reduces permeability of oxygen through the matrix. However, instability of the fiber surface coating and possible fiber degradation still results in some loss in composite strength.

SUMMARY AND CONCLUSIONS

A strong, tough, and therefore more reliable silicon-based ceramic composite can be fabricated by reinforcing RBSN with high strength, high modulus, continuous length SiC fibers. The important features of this composite are as follows.

1. In the tensile mode, the room temperature strength properties of unidirectional composites showed no influence of tested volume or artificial notches, and were unaffected by quenching from temperatures up to 1100 °C. These all
indicate excellent toughness or flaw resistance for the composite material.

2. In the bend mode, the unidirectional composites retained their as-fabricated fast-fracture ultimate strength to 1200 °C in oxygen.

3. In a nitrogen environment, the unidirectional composites displayed excellent thermal stability after 100 hr exposure at temperatures to 1400 °C.

4. In an oxidizing environment, the composite retained nearly 60 percent of its as-fabricated strength after 100 hr exposure at 1200 and 1400 °C. However, those heat treated between 400 and 1200 °C showed strength loss due to oxidation of the interfacial region, the porous silicon nitride matrix, and the SiC fibers.

Because of their good strength properties, notch insensitivity, and thermal shock resistance, SiC/RBSN composites are potential candidates for high temperature applications such as heat engines. Further improvement in composite properties are needed, however, to avoid long-term oxidation induced degradation. This may be achievable by fully densifying the matrix and/or by providing a dense coating for the composite surface.

REFERENCES

1. Buljan, S.T.; and Sarin, V.K.: Silicon Nitride Based Composites. Composites, vol. 18, no. 2, Apr. 1987, pp. 99-106.

2. Mah, T.; Mendiratta, M.G.; and Lipsitt, H.A.: Fracture Toughness and Strength of Si_3N_4-TiC Composites. Am. Ceram. Soc. Bull., vol. 60, no. 11, Nov. 1981, pp. 1229-1231,1240.

3. DiCarlo, J.A.; and Williams, W.: Dynamic Modulus and Damping of Boron, Silicon Carbide, and Alumina Fibers. NASA TM-81422, 1980.

4. Bhatt, R.T.: Mechanical Properties of SiC Fiber Reinforced Reaction-Bonded Si_3N_4 Composites. Tailoring Multiphase and Composite Ceramics, R.E. Tressler, et al., eds., Plenum Press, 1986, pp. 675-686.

5. Bhatt, R.T.: Effect of Fabrication Conditions on the Properties of SiC Fiber Reinforced Reaction-Bonded Silicon Nitride Matrix Composites. NASA TM-88814, 1986.

6. Aveston, J.; Cooper, G.A.; and Kelley, A.: Single and Multiple Fracture. The Properties of Fibre Composites, IPC Science and Technology Press Ltd., Surrey, England, 1971, pp. 15-26.

7. Fracture Toughness. ISI Publication 121, The Iron and Steel Institute, London, 1968.

8. Bansal, G.K.; and Duckworth, W.H.: Effects of Specimen Size on Ceramic Strengths. Fracture Mechanics of Ceramics, Vol. 3, R.C. Bradt, D.P.H. Hasselman, and F.F. Lange, eds., Plenum Press, 1978, pp. 189-204.

9. Herrmansson, L.; Adlerborn, J.; and Burstrom, M.: Tensile Testing of Ceramic Materials - A New Approach. ASEA CERAMA AB Company, Internal Communication.

10. Vaidanathan, R.; Shankar, J.; and Avva, V.S.: Testing and Evaluation of Si_3N_4 in Uniaxial Tension at Room Temperature. Proceedings of the Twenty-Fifth Automotive Technology Development Contractors' Coordination Meeting, SAE, 1987, pp. 175-186.

11. Larsen, D.C., et al., eds.: Ceramic Materials for Advanced Heat Engines, Technical and Economic Evaluation. Noyes Publications, 1985.

12. Larsen, D.C.; Stuchly, S.L.; and Adams, J.W.: Evaluation of Ceramics and Ceramic Composites for Turbine Engine Applications. AFWAL Contract F33615-85-C-5101, Interim Technical Report No. 17, Sept. 1984.

13. Bhatt, R.T.: Oxidation Effects on the Mechanical Properties of SiC Fiber Reinforced Reaction-Bonded Silicon Nitride Composites (SIC/RBSN). To be published.

TABLE I. - ROOM TEMPERATURE MECHANICAL PROPERTIES FOR $[0]_8$ AND $[0/90]_S$ SiC/RBSN COMPOSITES ($V_f \sim 0.3$)

Properties	$[0]_8$	$[0/90]_S$
Elastic modulus, GPa	193±7	124±6
First matrix cracking strength, MPa	227±41	127±26
Composite ultimate strength, MPa	682±150	294±87
First matrix cracking strain, %	0.11	0.1
Composite ultimate fracture strain, %	0.45	0.6
Interfacial shear strength, MPa	18	------
In-plane shear modulus, GPa	31±2	------
In-plane shear strength, MPa	40	------
Fracture toughness, MPa$\sqrt{m}$	13	------

TABLE II. - ROOM TEMPERATURE STRENGTH PROPERTIES FOR UNNOTCHED AND NOTCHED $[0]_8$ AND $[0/90]_S$ SiC/RBSN COMPOSITES ($V_f \sim 0.3$)

Condition	$[0]_8$		$[0/90]_S$	
	First matrix cracking stress, MPa	Ultimate tensile strength, Mpa	First matrix cracking stress, MPa	Ultimate tensile strength, MPa
Unnotched	227±41	686±150	127±26	294±87
Single notched[a]	[b]201±12	[b]620±145	------	------
Double notched[a]	[b]226±15	[b]659±135	[b]151	[b]265

[a]Notch length, 3.00 mm; specimen width, 12 mm.
[b]Strength measured based on net cross-sectional area.

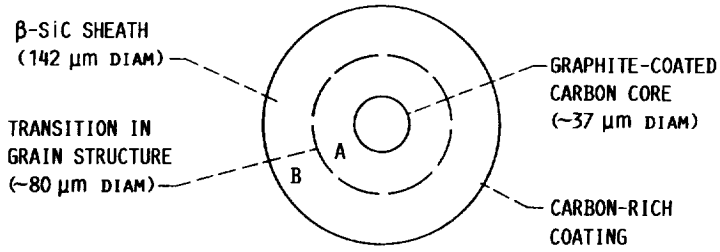

(a) SCHEMATIC OF CROSS SECTION OF FIBER.

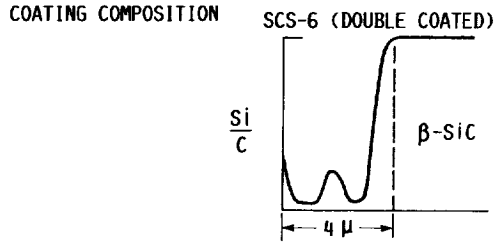

(b) COMPOSITION PROFILE OF CARBON-RICH COATING ON FIBER SURFACE (TEXTRON SCS-6).

FIGURE 1. - DETAILS OF CVD SiC FIBER.

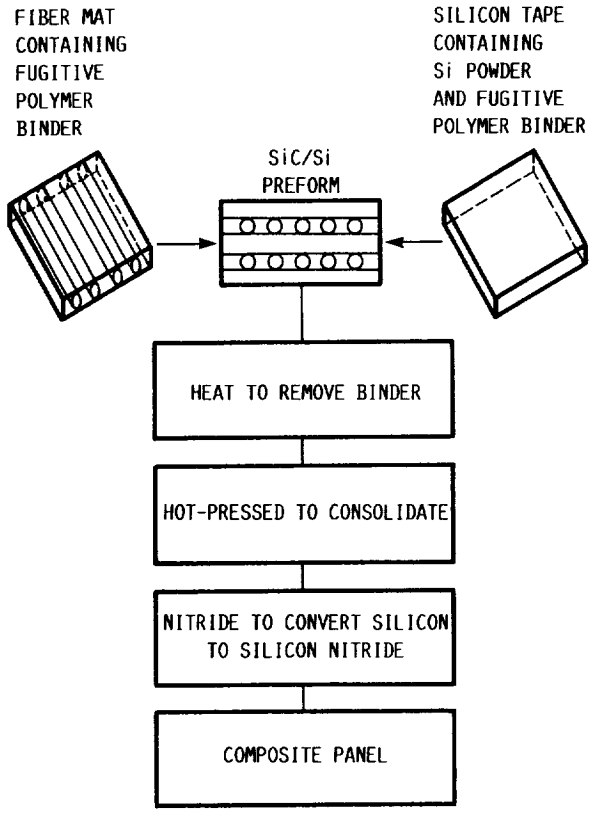

FIGURE 2. - BLOCK DIAGRAM SHOWING THE SiC/RBSN COMPOSITE FABRICATION PROCESS.

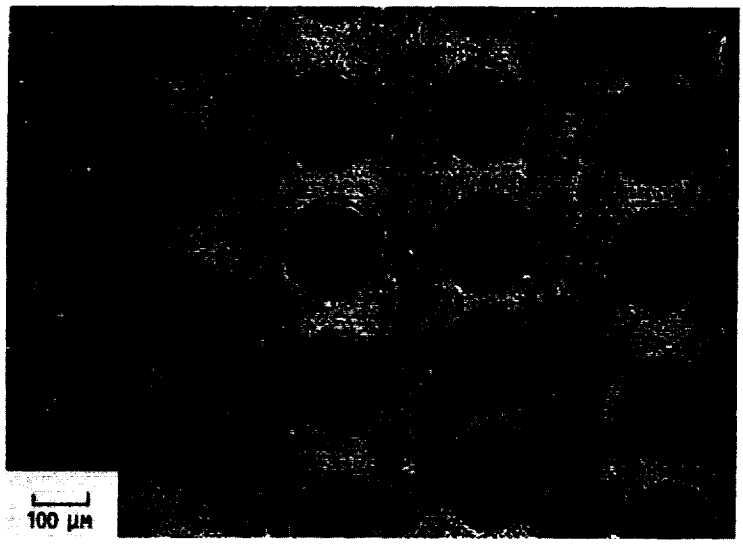

FIGURE 3. - A TYPICAL CROSS-SECTION OF A UNIDIRECTIONALLY REINFORCED SiC/RBSN COMPOSITE ($V_f \sim 0.3$).

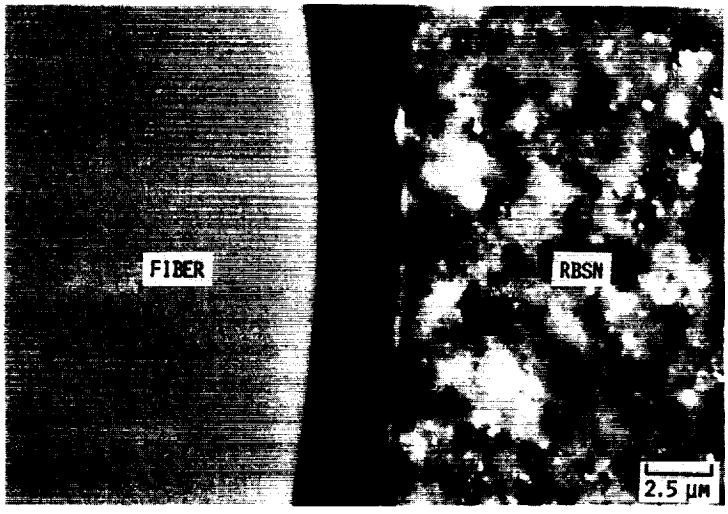

FIGURE 4. - PHOTOMICROGRAPH SHOWING THE INTERFACIAL REGION IN SiC/RBSN COMPOSITES.

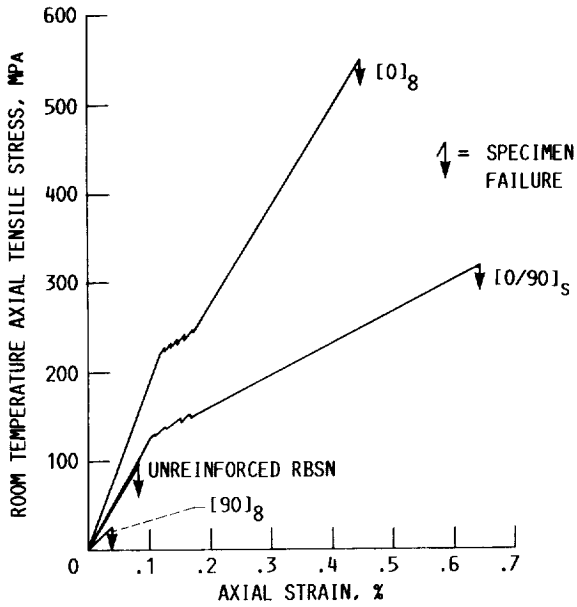

FIGURE 5. - TYPICAL STRESS-STRAIN CURVES FOR $[0]_8$, $[0/90]_S$, $[90]_8$ COMPOSITES, AND REINFORCED RBSN.

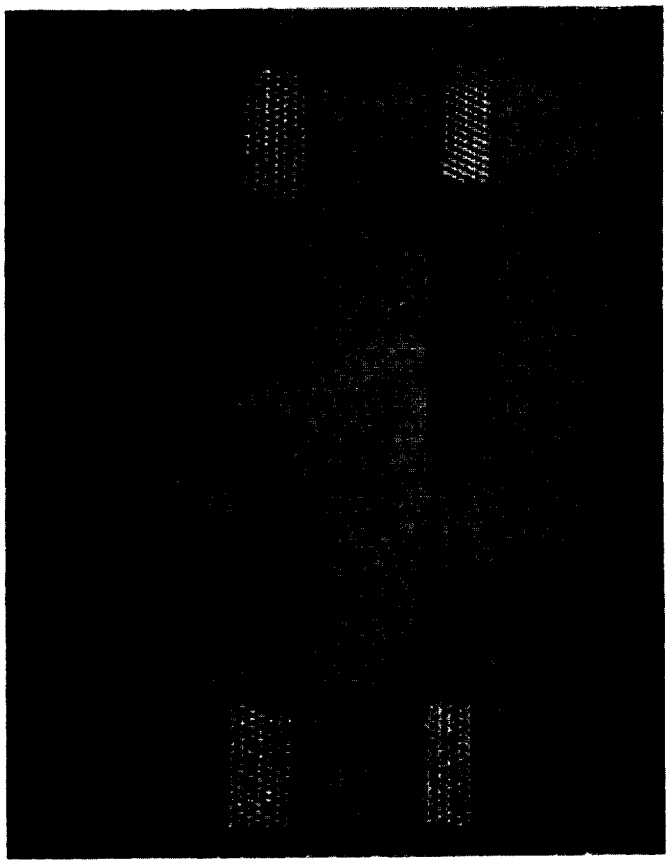

(a) (b)

FIGURE 6. - FRACTURED TENSILE SPECIMENS OF (a) $[0]_8$ AND (b) $[0/90]_S$ COMPOSITES SHOWING BRUSH-LIKE FRACTURE.

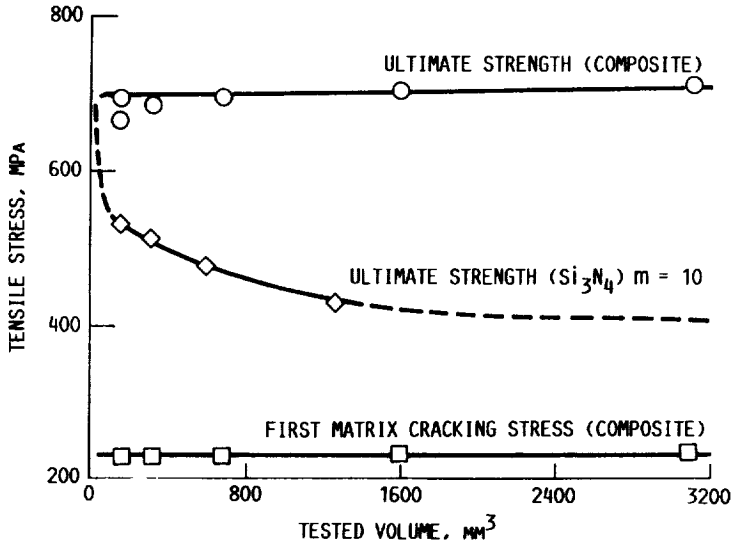

FIGURE 7. - VARIATION OF ROOM TEMPERATURE TENSILE PROPERTIES WITH TESTED VOLUME FOR UNIDIRECTIONALLY REINFORCED SiC/RBSN COMPOSITES ($V_f \sim 0.3$) AND MONOLITHIC Si_3N_4 [9,10].

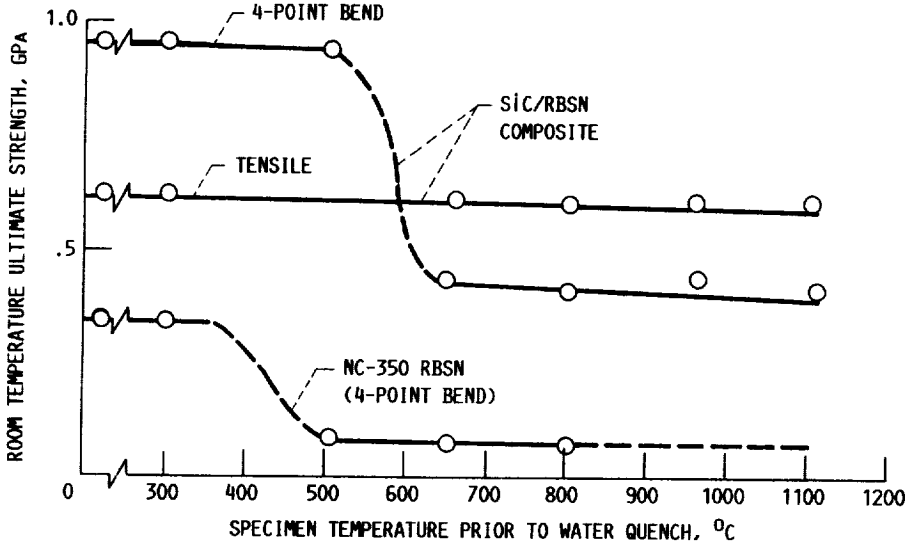

FIGURE 8. - THE ROOM TEMPERATURE TENSILE AND 4-POINT BEND STRENGTHS FOR UNIDIRECTIONALLY REINFORCED SiC/RBSN COMPOSITES ($V_f \sim 0.3$) AND MONOLITHIC RBSN (NC-350) AFTER QUENCHING FROM INDICATED TEMPERATURES.

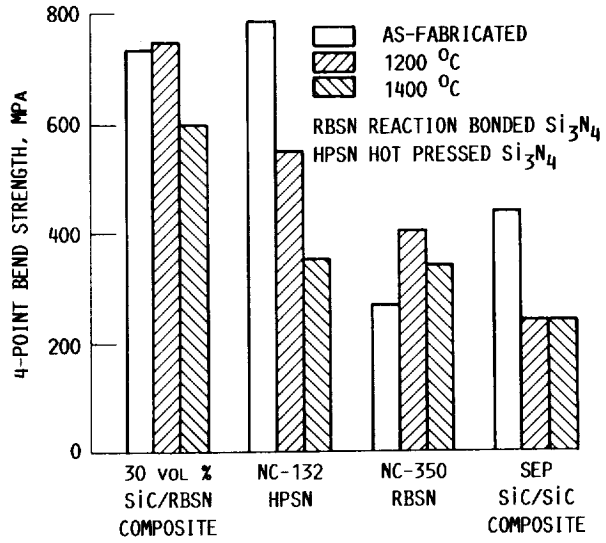

FIGURE 9. - BAR GRAPH SHOWING BEND STRENGTHS FOR UNIDIRECTIONALLY REINFORCED SiC/RBSN COMPOSITES ($V_f \sim 0.3$), HOT PRESSED Si_3N_4 RBSN (NC-350) AND 1-D SEP SiC/SiC COMPOSITES AT 25, 1200, AND 1400 °C.

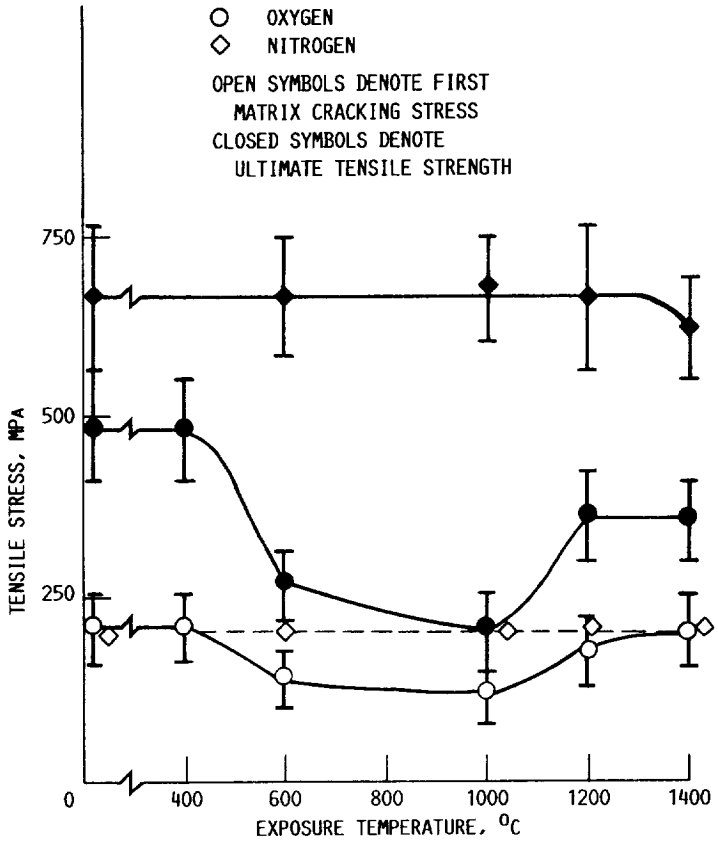

FIGURE 10. - ROOM TEMPERATURE TENSILE STRENGTHS FOR UNIDIRECTIONALLY REINFORCED SiC/RBSN COMPOSITES ($V_f \sim 0.3$) AFTER 100 HR EXPOSURE AT TEMPERATURES TO 1400 °C IN NITROGEN AND IN OXYGEN ENVIROMENTS.

NASA
National Aeronautics and Space Administration

Report Documentation Page

1. Report No.	2. Government Accession No.	3. Recipient's Catalog No.
NASA TM-101356 AVSCOM TR-88-C-027		

4. Title and Subtitle

Properties of Silicon Carbide Fiber-Reinforced Silicon Nitride Matrix Composites

5. Report Date

6. Performing Organization Code

7. Author(s)

Ramakrishna T. Bhatt

8. Performing Organization Report No.

E-4386

9. Performing Organization Name and Address

NASA Lewis Research Center
Cleveland, Ohio 44135-3191
and
Propulsion Directorate
U.S. Army Aviation Research and Technology Activity—AVSCOM
Cleveland, Ohio 44135-3127

10. Work Unit No.

535-07-01

11. Contract or Grant No.

12. Sponsoring Agency Name and Address

National Aeronautics and Space Administration
Washington, D.C. 20546-0001
and
U.S. Army Aviation Systems Command
St. Louis, Mo. 63120-1798

13. Type of Report and Period Covered

Technical Memorandum

14. Sponsoring Agency Code

15. Supplementary Notes

Presented at the International Conference on Whisker- and Fiber-Toughened Ceramics, sponsored by the American Society for Metals, Oak Ridge, Tennessee, June 6-9, 1988.

16. Abstract

The mechanical properties of NASA Lewis developed SiC/RBSN composites and their thermal and environmental stability have been studied. The composites consist of neary 30 vol% of aligned 142 μm diameter chemically vapor-deposited SiC fibers in a relatively porous silicon nitride matrix. In the as-fabricated condition, the unidirectional and 2-D composites exhibited metal-like stress-strain behavior, graceful failure, and showed improved properties when compared with unreinforced matrix of comparable density. Furthermore, the measured room temperature tensile properties were relatively independent of tested volume and were unaffected by artificial notches normal to the loading direction or by thermal shocking from temperatures up to 800 °C. The four-point bend strength data measured as a function of temperature to 1400 °C in air showed that as-fabricated strength was maintained to 1200 °C. At 1400 °C, however, nearly 15 percent loss in strength was observed. Measurement of room temperature tensile strength after 100 hr exposure at temperatures to 1400 °C in a nitrogen environment indicated no loss from the as-fabricated composite strength. On the other hand, after 100 hr exposure in flowing oxygen at 1200 °C and 1400 °C, the composites showed ~40 percent loss from their as-fabricated ultimate tensile strength. Those exposed between 400°-1200 °C showed nearly 60 percent strength loss. Oxidation of the fiber/matrix interface as well as internal oxidation of the porous Si_3N_4 matrix are likely mechanisms for strength degradation. The excellent strength reproducibility, notch insensitivity, and high temperature strength of the composite makes it an ideal candidate for advanced heat engine applications provided coating or densification methods are developed to avoid internal oxidation attack.

17. Key Words (Suggested by Author(s))	18. Distribution Statement
Ceramic fiber reinforced ceramic matrix composites; Fiber toughened composites; SiC fiber Si_3N_4 matrix; Mechanical and physical properties	Unclassified – Unlimited Subject Category 24

19. Security Classif. (of this report)	20. Security Classif. (of this page)	21. No of pages	22. Price*
Unclassified	Unclassified	16	A02

NASA FORM 1626 OCT 86

*For sale by the National Technical Information Service, Springfield, Virginia 22161